ENGINEERING RESEARCH INSTITUTE
THE UNIVERSITY OF MICHIGAN
ANN ARBOR

Progress Report 1

PART I. SOME STUDIES OF TRANSISTOR MEASUREMENT TECHNIQUES AT HIGH FREQUENCIES

P. M. Shaler, Jr.

PART II. GAS-TUBE STUDY

W. P. Brown

Approved by:

N. W. Spencer
Project Supervisor

ERI Project 2269

DEPARTMENT OF THE ARMY
DIAMOND ORDNANCE FUZE LABORATORIES
CONTRACT NO. DAI-49-186-502-ORD(P)-194
WASHINGTON, D. C.

February 1958

PERSONNEL EMPLOYED DURING THE PERIOD OF THE REPORT

P. M. Shaler, Jr.	Project Engineer	Three-quarter time, student
R. G. DeLosh	Student Technician	Part time
W. P. Brown	Student Engineer	Part time
N. W. Spencer	Supervisor	Part time
W. G. Dow	Consultant	

TABLE OF CONTENTS

LIST OF FIGURES

LIST OF FIGURES (Concluded)

PART I

ABSTRACT

Studies related to measurements of the external properties of transistors have led to techniques for the predictions of current gain 3-db cutoff frequencies, and of internal properties associated with a suggested equivalent circuit.

OBJECTIVE

The purpose of this investigation is to find methods for determining the internal properties of transistors designed for operation in the VHF and UHF frequency ranges through measurement of their external properties.

1. INTRODUCTION

This progress report refers to the beginning phase of a new task under Contract No. DAI-49-186-502-ORD(P)-194, with the purpose of investigating instrumentation requirements and devising suitable instrumentation techniques for the experimental study and evaluation of very-high-frequency semiconductor devices.

A particular objective is to evaluate very-high-frequency transistors in terms of measurements of their externally measurable parameters as represented, for example, by an equivalent circuit. Work has been done which will first enable the measurement and understanding of transistors whose limitations become apparent at frequencies much lower than those in the VHF range. Following this, investigations will be confined largely to frequencies above 100 mcs.

Thus this report summarizes these efforts, which include associated analytical review of low-frequency equivalent circuits, H parameters, some experimentation with oscillators at higher frequencies, and finally measurements of some input and output impedance under various conditions.

2. CHARACTERISTICS OF LOW-FREQUENCY TRANSISTORS

To gain familiarity with the external characteristics of low-frequency transistors, an experiment was carried out involving the measurement of impedance and of gain versus frequency. Using a grounded base configuration, a relationship between α and frequency was obtained which verified that the gain cutoff curve had a slope of 6 db/octave (at about 300 kcs). Then $R_{in_{GB}}$ (the input resistance of a grounded base amplifier) and its dependence on I_e were measured. Also, by noting resonance effects, measurements were made of collector capacitance C_c, as a function of collector voltage V_{CB}, which verified that an alloy junction transistor has an effective capacitance inversely proportional to the square root of V_C. Using a grounded emitter configuration, a curve was prepared of the grounded emitter current gain β versus frequency for a transistor, and the 3-db gain drop-off was observed to occur so that:

$$f_\beta \approx (1-a)f_\alpha \quad . \tag{2.1}$$

The input resistance of a grounded emitter amplifier $R_{in_{GE}}$ was then measured to verify that:

$$R_{in_{GE}} \approx \frac{R_{in_{GB}}}{(1-a)} \quad . \tag{2.2}$$

3. SMALL SIGNAL A-C EQUIVALENT CIRCUIT PARAMETERS

Recognizing the need for a mathematical model to represent the transistor, reference was made to a paper[1] concerning the general active a-c equivalent circuit. This paper contains a discussion which deals with loop- and nodal-derived equivalent circuits, and terminates with tables of transformation formulas useful for converting any loop-derived equivalent circuit into any T configuration, or any nodal-derived equivalent circuit into any π configuration. The equations of interest concerning T equivalent configurations have the form:

$$V_1 = Z_{11} I_1 + Z_{12} I_2 \; ; \tag{3.1}$$

$$V_2 = Z_{21} I_1 + Z_{22} I_2 \; . \tag{3.2}$$

The quantities Z_{11}, Z_{22}, Z_{12}, and Z_{21} are open-circuit impedances; for example, Z_{11} is equal to the ratio V_1/I_1 with the output open-circuited, i.e., $I_2 = 0$.

$$Z_{11} = \frac{V_1}{I_1} \quad (\text{for } I_2 = 0) \; , \tag{3.3}$$

$$Z_{12} = \frac{V_1}{I_2} \quad (\text{for } I_1 = 0) \; , \tag{3.4}$$

$$Z_{21} = \frac{V_2}{I_1} \quad (\text{for } I_2 = 0) \; , \text{ and} \tag{3.5}$$

$$Z_{22} = \frac{V_2}{I_2} \quad (\text{for } I_1 = 0) \; . \tag{3.6}$$

If one knows the four open-circuit parameters Z_{11}, Z_{12}, Z_{21}, and Z_{22} for a grounded base transistor configuration, one can use the transformation tables to find a new set of open-circuit parameters for either a grounded emitter or grounded collector configuration.

The equations concerning π equivalent configurations are:

$$I_1 = Y_{11} V_1 + Y_{12} V_2 \quad \text{and} \tag{3.7}$$

$$I_2 = Y_{21} V_1 + Y_{22} V_2 \; . \tag{3.8}$$

The quantities Y_{11}, Y_{12}, Y_{21}, and Y_{22} are short-circuit admittances:

$$Y_{11} = \frac{I_1}{V_1} \quad (\text{for } V_2 = 0) \quad , \tag{3.9}$$

$$Y_{12} = \frac{I_1}{V_2} \quad (\text{for } V_1 = 0) \quad , \tag{3.10}$$

$$Y_{21} = \frac{I_2}{V_1} \quad (\text{for } V_2 = 0) \quad , \text{ and} \tag{3.11}$$

$$Y_{22} = \frac{I_2}{V_2} \quad (\text{for } V_1 = 0) \quad . \tag{3.12}$$

As before, once the short-circuit admittance parameters are known for one of the transistor configurations, transformations will allow the new parameters to be obtained for either of the remaining configurations.

3.1 THE EQUIVALENCE OF THE T AND π REPRESENTATION

The equivalence between the T and π representations of a particular transistor configuration can be shown as follows. If the open-circuit parameters for a T configuration are known, the short-circuit parameters for an equivalent π of the same active circuit are:

$$Y_{11} = \frac{Z_{22}}{Z_{11} Z_{22} - Z_{12} Z_{21}} \quad , \tag{3.13}$$

$$Y_{21} = \frac{-Z_{21}}{Z_{11} Z_{22} - Z_{12} Z_{21}} \quad , \tag{3.14}$$

$$Y_{12} = \frac{-Z_{12}}{Z_{11} Z_{22} - Z_{12} Z_{21}} \quad , \text{ and} \tag{3.15}$$

$$Y_{22} = \frac{Z_{11}}{Z_{11} Z_{22} - Z_{12} Z_{21}} \quad . \tag{3.16}$$

If the short-circuit parameters for a π configuration are known, the open-circuit parameters for an equivalent T of the same active circuit are:

$$Z_{11} = \frac{Y_{22}}{Y_{11} Y_{22} - Y_{12} Y_{21}} \quad , \tag{3.17}$$

$$Z_{21} = \frac{-Y_{21}}{Y_{11}\,Y_{22} - Y_{12}\,Y_{21}} \quad , \tag{3.18}$$

$$Z_{12} = \frac{-Y_{12}}{Y_{11}\,Y_{22} - Y_{12}\,Y_{21}} \quad , \text{ and} \tag{3.19}$$

$$Z_{22} = \frac{Y_{11}}{Y_{11}\,Y_{22} - Y_{12}\,Y_{21}} \quad . \tag{3.20}$$

3.2 A METHOD OF DETERMINING Y AND Z PARAMETERS IF THE H PARAMETERS ARE KNOWN

Because of ease of measurement, H parameters are often used to represent the "black box" active circuit. The equations of interest are:

$$V_1 = h_{11}I_1 + h_{12}V_2 \quad , \tag{3.21}$$

$$I_2 = h_{21}I_1 + h_{22}V_2 \quad , \tag{3.22}$$

$$h_{11} = \frac{V_1}{I_1} \quad (\text{for } V_2 = 0) \quad , \tag{3.23}$$

$$h_{12} = \frac{V_1}{V_2} \quad (\text{for } I_1 = 0) \quad , \tag{3.24}$$

$$h_{21} = \frac{I_2}{I_1} \quad (\text{for } V_2 = 0) \quad , \text{ and} \tag{3.25}$$

$$h_{22} = \frac{I_2}{V_2} \quad (\text{for } I_1 = 0) \quad . \tag{3.26}$$

If the H parameters for an active circuit configuration are known, the open-circuit parameters for an equivalent T of the same configuration are:

$$Z_{11} = h_{11} - \frac{h_{12}h_{21}}{h_{22}} \quad , \tag{3.27}$$

$$Z_{12} = \frac{h_{12}}{h_{22}} \quad , \tag{3.28}$$

$$Z_{21} = -\frac{h_{21}}{h_{22}} \quad , \text{ and} \tag{3.29}$$

$$Z_{22} = \frac{1}{h_{22}} \quad . \tag{3.30}$$

If the short-circuit parameters for an equivalent π of the same configuration are preferred:

$$Y_{11} = \frac{1}{h_{11}} , \tag{3.31}$$

$$Y_{12} = -\frac{h_{12}}{h_{11}} , \tag{3.32}$$

$$Y_{21} = \frac{h_{21}}{h_{11}} , \text{ and} \tag{3.33}$$

$$Y_{22} = h_{22} - \frac{h_{12}h_{21}}{h_{11}} . \tag{3.34}$$

4. LOW-FREQUENCY CIRCUIT REPRESENTATION OF THE TRANSISTOR

A low-frequency equivalent circuit is shown in Fig. 4.1. It has been assumed that the frequency of operation is low enough so that the effect of the capacitive reactance due to C_c, the collector capacitance, can be neglected.

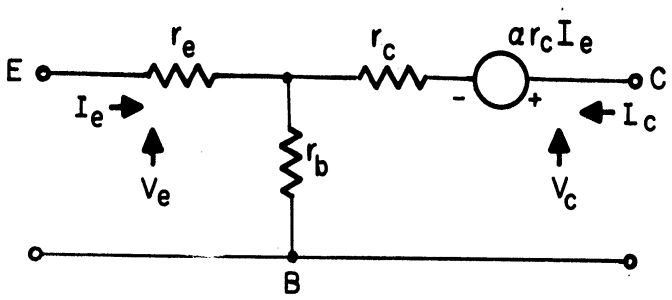

Fig. 4.1. Low-frequency equivalent circuit of the grounded base configuration.

r_e is the effective emitter resistance $\approx \frac{KT\ (mv)}{qI_e(ma)}$,

r_c is the effective collector resistance,

r_b is the effective low-frequency base resistance, and

α is the short-circuit current gain of the grounded base configuration.

The equations concerning this configuration are:

$$V_e = Z_{11}I_e + Z_{12}I_c \text{ and} \tag{4.1}$$

$$V_c = Z_{21}I_e + Z_{22}I_c . \tag{4.2}$$

The open-circuit parameters are:

$$Z_{11} = r_e + r_b \quad , \tag{4.3}$$

$$Z_{12} = r_b \quad , \tag{4.4}$$

$$Z_{21} = r_b + \alpha r_c \quad , \text{ and} \tag{4.5}$$

$$Z_{22} = r_b + r_c \quad . \tag{4.6}$$

If H parameters have been measured for a particular transistor in the grounded base configuration and it is desired to obtain representation using the simplified low-frequency equivalent circuit, the transformations are as follows:

$$r_e = h_{11} - \frac{h_{12}\,(h_{21} + 1)}{h_{22}} \quad , \tag{4.7}$$

$$r_b = \frac{h_{12}}{h_{22}} \quad , \tag{4.8}$$

$$r_c = \frac{1 - h_{12}}{h_{22}} \approx \frac{1}{h_{22}} \quad , \text{ and} \tag{4.9}$$

$$\alpha = -\frac{h_{12} + h_{21}}{1 - h_{12}} \approx -h_{21} \quad . \tag{4.10}$$

4.1 HIGH-FREQUENCY CIRCUIT REPRESENTATION OF THE TRANSISTOR

The low-frequency representation applies only when it is known that inherent reactances can be neglected and that the phase shift of the collector current with respect to emitter current is negligible.

Middlebrook[2] accounts for high-frequency effects in a treatment involving admittance parameters. He has derived formulas for obtaining the four admittances after six basic measurements have been made. The representation of these parameters is in the form shown in Fig. 4.2. This elegant treatment is

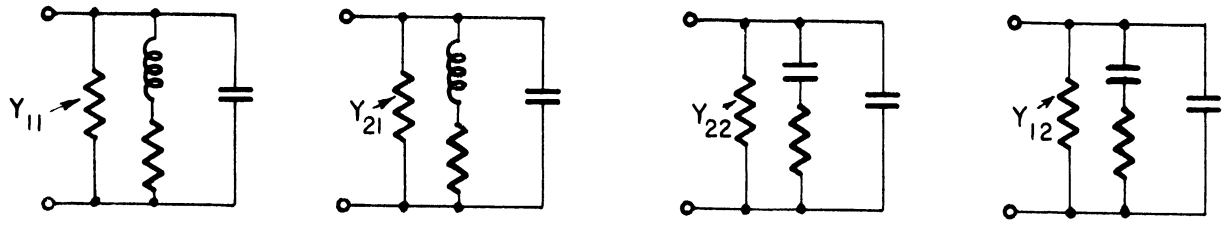

Fig. 4.2. Admittance forms as treated by Middlebrook.

more complete than the one by Shea[3] but is also more complicated. The principal high-frequency circuit effects as described by Shea are those of the collector capacitance, the base spreading resistance, and of the complex value of α.

Until it is necessary to do otherwise, the representation as described by Shea will be referred to in this report. The general form is shown in Fig. 4.3.

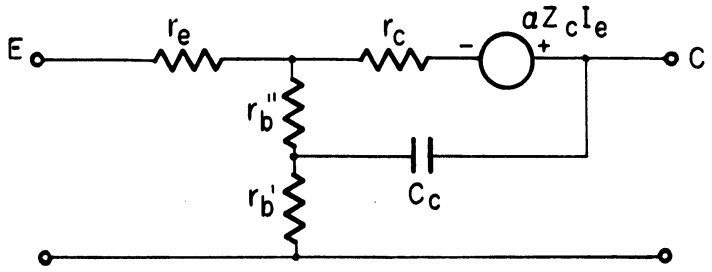

Fig. 4.3. Equivalent circuit of the grounded base configuration including r_b'', r_b', and C_c.

r_b' is the high-frequency base spreading resistance,

r_b'' is an apparent feed-back resistance due to the variation of the effective width of the base layer with collector voltage,

C_c is the capacitance of the space change or depletion layer at the collector junction, and

$\alpha = \dfrac{a_o}{1 + j(\omega/\omega_\alpha)}$, where a_o is the "zero frequency" current gain and ω_α is the radian frequency at which the magnitude of α drops to 0.707 a_o.

At higher frequencies, when the reactance of C_c is much smaller than r_c, the effects of r_b'' can usually be neglected. By including only the most important frequency effects, practical circuits for the three transistor configurations can thus be obtained.

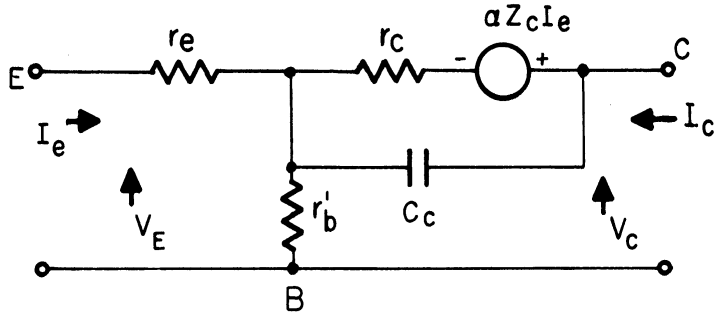

Fig. 4.4. High-frequency equivalent circuit for the grounded base configuration.

Summarizing, the grounded base case is as shown in Fig. 4.4. Where

$$Z_c = \frac{r_c}{1 + j\omega r_c C_c} , \tag{4.11}$$

the open-circuit parameters are:

$$Z_{11} = r_e + r_b' , \tag{4.12}$$

$$Z_{12} = r_b' , \tag{4.13}$$

$$Z_{21} = r_b' + \alpha Z_c , \text{ and} \tag{4.14}$$

$$Z_{22} = r_b' + Z_c . \tag{4.15}$$

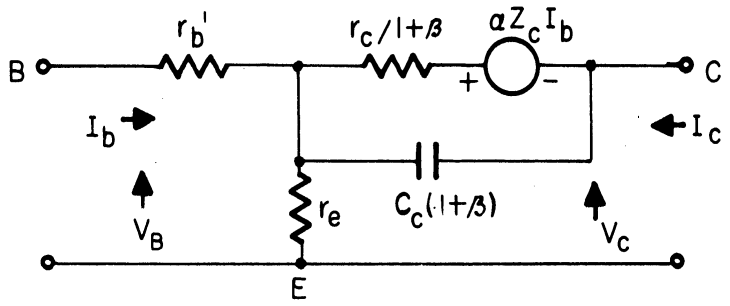

Fig. 4.5. High-frequency equivalent circuit for the grounded emitter configuration.

Similarly, the grounded emitter case is shown in Fig. 4.5. The short-circuit grounded emitter current gain is the ratio of I_c to I_b:

$$\beta = \frac{\alpha}{1 - \alpha} . \tag{4.16}$$

The open-circuit parameters are:

$$Z_{11} = r_b' + r_e , \tag{4.17}$$

$$Z_{12} = r_e , \tag{4.18}$$

$$Z_{21} = r_e - \alpha Z_c , \text{ and} \tag{4.19}$$

$$Z_{22} = r_e + \frac{Z_c}{1 + \beta} . \tag{4.20}$$

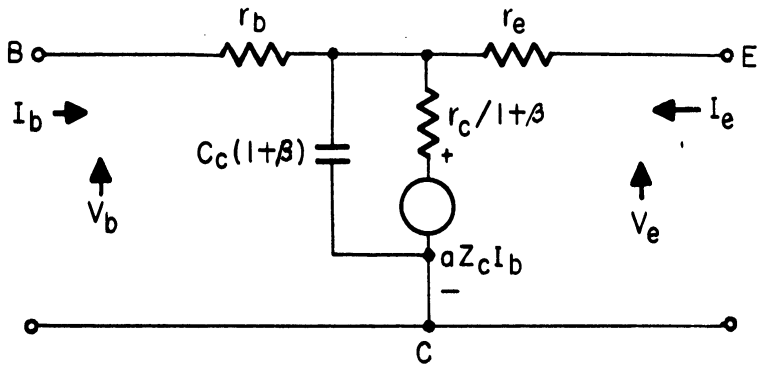

Fig. 4.6. High-frequency equivalent circuit for the grounded collector configuration.

Finally, the grounded collector is shown in Fig. 4.6. The open-circuit parameters are:

$$Z_{11} = r_b + Z_c \quad , \tag{4.21}$$

$$Z_{12} = \frac{Z_c}{1 + \beta} \quad , \tag{4.22}$$

$$Z_{21} = Z_c \quad , \text{ and} \tag{4.23}$$

$$Z_{22} = r_e + \frac{Z_c}{1 + \beta} \quad . \tag{4.24}$$

5. NONLINEAR OPERATION AND OSCILLATORS

For most purposes it is desirable to obtain a wave form which is reasonably sinusoidal; thus a brief review of the effects of inherent oscillator nonlinearity is desirable. Oscillations start in a region in which the emitter-base diode is conducting, and the collector-base diode is nonconducting. As the amplitude increases, one or the other of the two diodes will experience a reversal of polarity, thus limiting the amplitude of oscillations. If the collector becomes positive (for a PNP transistor), the collector-base diode will then become conducting. In general, this will short-circuit the high impedance or resonant part of the circuit. If the emitter, on the other hand, goes negative, the emitter-base diode becomes nonconducting, generally causing a voltage surge across the inductance in the circuit. Compensation for these effects can be obtained by inserting resistance in series with the collector and in parallel with the emitter to base junction.

A basic circuit useful for experimentation is shown in Fig. 5.1.

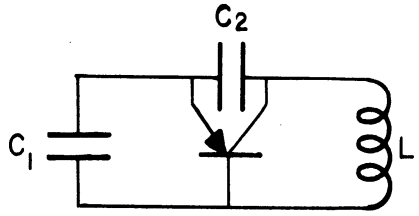

Fig. 5.1. A transistor oscillator circuit.

The frequency of oscillation can be determined from:

$$\omega^2 \approx \frac{1}{L}\left(\frac{C_1 + C_2}{C_1C_2 + C_1C_c + C_2C_c}\right) , \qquad (5.1)$$

where

$$C_2 = C_1 \frac{\alpha}{1 - \alpha} . \qquad (5.2)$$

Using a radio receiver to detect the generated signal, and varying the frequency of oscillations by controlling L, C_1, and C_2, f_{max} (the frequency at which the available power gain is no longer ≥ 1 can be determined.

For example, frequencies between 56 and 70 mcs were measured for type 2N128 transistors, between 70 and 79 mcs for type 2N129 transistors, and a maximum frequency of approximately 400 mcs for a type GA53233 diffused base transistor.

6. FORMULATIONS OF INPUT AND OUTPUT IMPEDANCE

The general four-terminal active network allowing the derivation of input and output impedance is shown in Fig. 6.1.

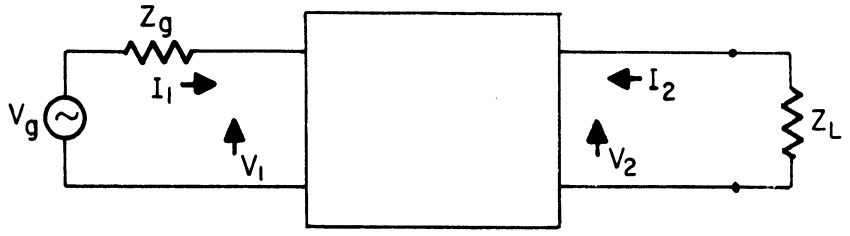

Fig. 6.1. The general four-terminal active network.

In general, the input and output impedances can be written as follows:

$$Z_i = Z_{11} - \frac{Z_{12}Z_{21}}{Z_{22} + Z_L} \quad \text{and} \tag{6.1}$$

$$Z_o = Z_{22} - \frac{Z_{12}Z_{21}}{Z_{11} + Z_g} \quad . \tag{6.2}$$

Applying the above relationships to the grounded base configuration, and referring to Fig. 4.3 and Eqs. (4.11) through (4.15):

$$Z_{i_{GB}} = r_e + r_b' \left[\frac{Z_c\,(1-\alpha) + Z_L}{r_b' + Z_L + Z_c}\right] \quad \text{and} \tag{6.3}$$

$$Z_{o_{GB}} = Z_c \left[1 - \frac{\alpha r_b'}{r_e + r_b' + Z_g}\right] + \frac{r_b'\,(r_e + Z_g)}{r_e + r_b' + Z_g} \quad . \tag{6.4}$$

At lower frequencies where the reactance of Z_c is much greater than $Z_L + r_b'$ and $Z_c(1-\alpha)$ is much greater than Z_L, $Z_{i_{GB}}$ can be simplified:

$$Z_{i_{GB}} \approx r_e + r_b'(1-\alpha) \;, \quad Z_c \gg (r_b' + Z_L) \;, \quad Z_c(1-\alpha) > Z_L \;. \tag{6.5}$$

If Z_g is short-circuited and if the parallel combination of r_b' and r_e is negligibly small, which is generally the case, Z_o can be simplified:

$$Z_{o_{GB}} \approx Z_c \left[1 - \frac{\alpha r_b'}{r_e + r_b'}\right], \quad Z_g = 0 \quad . \tag{6.6}$$

If, on the other hand, Z_g is made very large in comparison to r_b', which in turn is much greater than r_e, Z_o can be simplified another way:

$$Z_{o_{GB}} \approx Z_c + r_b' \;, \quad Z_g \gg r_b' > r_e \quad . \tag{6.7}$$

Note here that $Z_{o_{GB}}$ is shown in two forms depending upon the magnitude of Z_g.

In like manner the relationships for the grounded emitter configuration can be obtained:

$$Z_{i_{GE}} = r_b' + r_e \left[\frac{Z_c + Z_L}{r_e + Z_c(1-\alpha) + Z_L}\right] \quad \text{and} \tag{6.8}$$

$$Z_{o_{GE}} = Z_c(1-\alpha) + r_e \left[\frac{r_b' + Z_g + \alpha Z_c}{r_b' + Z_g + r_e}\right] \quad . \tag{6.9}$$

If the load impedance is so small that the reactive part of $Z_c(1-\alpha)$ is much greater than $(Z_L + r_e)$ in the range of the frequencies used, Z_i can be simplified:

$$Z_{i_{GE}} \approx r_b' + r_e \frac{1}{(1-\alpha)} = r_b' + r_e (1+\beta) \quad , \tag{6.10}$$

$$Z_c(1-\alpha) \gg (Z_L + r_e) \quad .$$

To study the variation of $Z_{o_{GE}}$ with frequency, neglect $(r_b' + Z_g)$ in comparison with αZ_c in Eq. (6.9) and consider:

$$Z_{o_{GE}} \approx (1 + K\alpha - \alpha) Z_c \quad , \qquad K = \frac{r_e}{Z_g + r_b' + r_e} \quad . \tag{6.11}$$

The order of magnitude of r_e is about one-tenth of r_b', and if Z_g is ten times as great as r_b', the value of K is about 0.01. When the magnitude of $(1-\alpha)$ is much greater than 0.01, this value of K can be neglected and Eq. (6.11) yields:

$$Z_{o_{GE}} \approx Z_c(1-\alpha) = Z_c \frac{1}{(1+\beta)} \quad , \qquad Z_g > r_b' > r_e \quad . \tag{6.12}$$

Finally, the relationships for the grounded collector configuration can be obtained:

$$Z_{i_{GC}} = r_b' + Z_c \left[\frac{r_e + Z_L}{r_e + Z_L + Z_c/1+\beta} \right] \quad , \text{ and} \tag{6.13}$$

$$Z_{o_{GC}} = r_e + \frac{Z_c}{1+\beta} \left[\frac{r_b' + Z_g}{r_b' + Z_g + Z_c} \right] \quad . \tag{6.14}$$

If a resistive load is used so that R_L is much greater than r_e, the form of Z_i becomes:

$$Z_{i_{GC}} \approx r_b' + Z_c \left[\frac{R_L}{R_L + Z_c/1+\beta} \right] = r_b' + \frac{Z_c R_L (1+\beta)}{Z_c + R_L (1+\beta)} \quad . \tag{6.15}$$

The form of Eq. (6.15) represents a resistance r_b' in series with the parallel combination of $R_L(1+\beta)$ and Z_c.

If the frequency of operation is such that Z_c is much greater than $(r_b' + Z_g)$, Z_o can be simplified:

$$Z_{o_{GC}} \approx r_e + \frac{r_b' + Z_g}{1 + \beta} \quad . \tag{6.16}$$

7. OUTPUT IMPEDANCE OF THE GROUNDED BASE AND GROUNDED EMITTER CONFIGURATIONS

The grounded emitter and grounded base configurations are of interest considering output impedance measurements because of the inherent dependency of Z_o upon Z_c. These impedances will have a greater magnitude than those of the grounded collector configuration, which are primarily dependent upon Z_g (Z_g being much smaller than Z_c). Also, the magnitude of $Z_{o_{GB}}$ and $Z_{o_{GE}}$ can be expected to decrease with an increase in the frequency of measurement because of the shunt capacitive reactance of Z_c, whereas the magnitude of $Z_{o_{GC}}$ can be expected to increase with frequency due to the decrease in the magnitude of $(1+\beta)$ which appears in the denominator in the expression for $Z_{o_{GC}}$.

From the grounded base configuration, information can be obtained making use of Eqs. (6.6) and (6.7):

$$Z_{o1} \approx Z_c + r_b' \qquad Z_g \gg r_b' > r_e \tag{7.1}$$

$$Z_{o2} \approx Z_c \left(1 - \frac{\alpha r_b'}{r_e + r_b'}\right) \qquad Z_g \approx 0 \quad . \tag{7.2}$$

To this end, measurements were made using the circuit of Fig. 7.1.

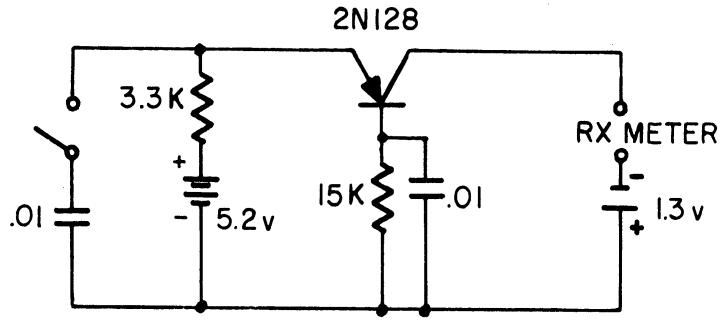

Fig. 7.1. Circuit for measurement of Z_{o1} and Z_{o2}.

Z_{o1} was measured with the switch open and Z_{o2} with the switch closed. Curves showing the resulting magnitude and phase angle of the impedance versus frequency are shown in Fig. 7.2.

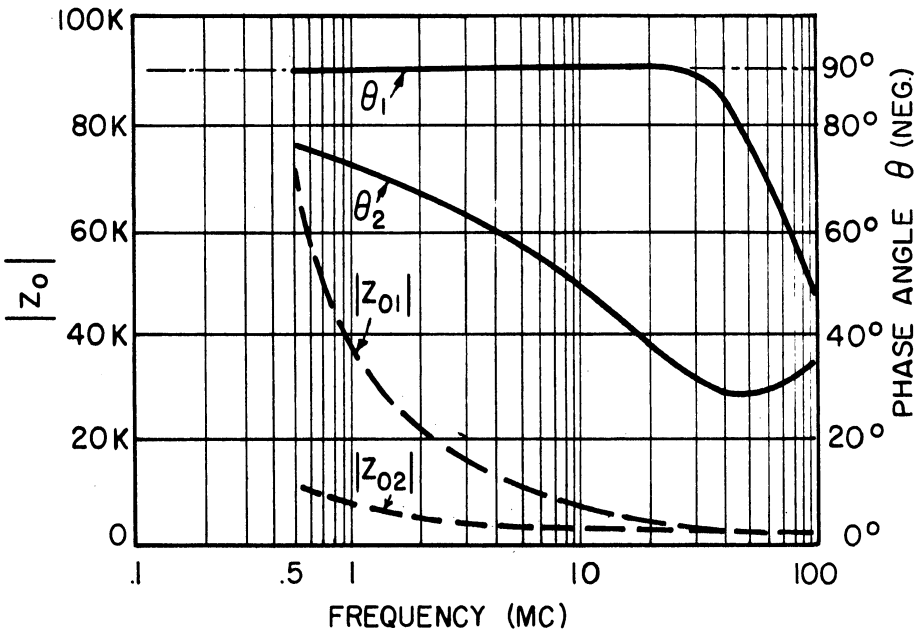

Fig. 7.2. Curves of $|Z_{01}|$ $\angle\theta_1$ and $|Z_{02}|$ $\angle\theta_2$ versus frequency for a type 2N128 transistor.

Observing the curves of Fig. 7.2, one notes that the phase shift of Z_{01} is approximately 90° at lower frequencies and then decreases at higher frequencies. Z_c is primarily capacitive because the frequencies of operation are much higher than the frequency associated with one r_cC_c time constant (at which the phase shift is 45°). At higher frequencies, the reactance of C_c approaches the magnitude of the series resistance r_b', and thus the decrease in phase shift would be expected. A more thorough treatment of the effect of r_b' on Z_{OGB} at high frequencies will be found in Section 8 of this report.

One will notice also that the phase shift of Z_{02} is always less than that of Z_{01}. This is due to the complex α. After the curves of the output impedance of the grounded emitter configuration have been discussed, the reason for this relationship will become clearer.

From the grounded emitter configuration, information can be obtained making use of Eq. (6.12):

$$Z_{03} \approx Z_c(1-\alpha) = Z_c \frac{1}{(1+\beta)}, \quad Z_g > r_b' . \tag{7.3}$$

Measurements were made using the circuit of Fig. 7.3. In this regard, note that if the switch in Fig. 7.3 is closed, the circuit is identical with that shown in Fig. 7.1 also with the switch closed, and the conditions for measurement of Z_{02} are met. Z_{03} was determined with the switch in the circuit shown in Fig. 7.3 open. Curves showing the magnitude and phase angle of impedance versus frequency are shown in Fig. 7.4 for both Z_{03} and Z_{02}, using a lower scale than in Fig. 7.2 to allow further comparison.

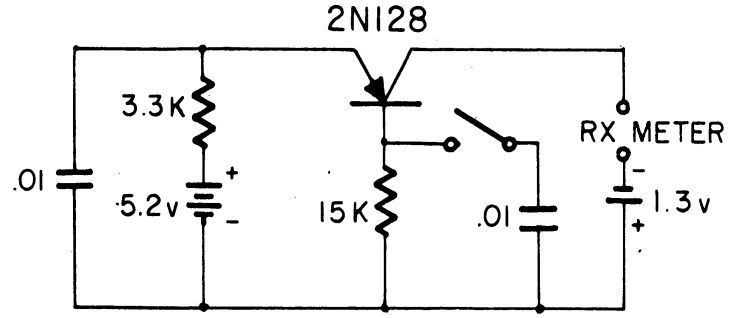

Fig. 7.3. Circuit for measurement of Z_{03} or Z_{02}.

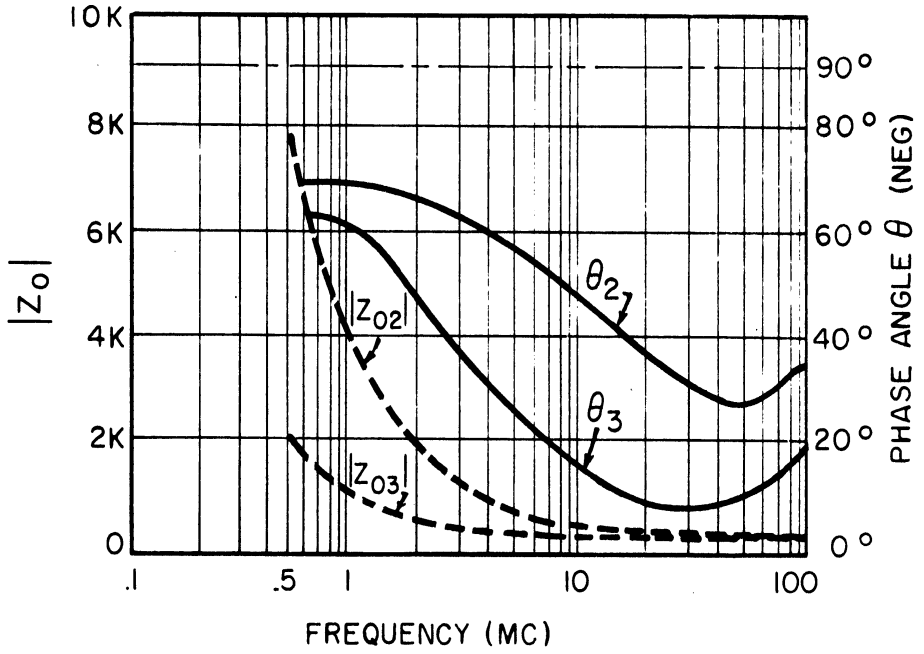

Fig. 7.4. Curves of $|Z_{02}|$ $\angle\theta_2$ and $|Z_{03}|$ $\angle\theta_3$ versus frequency for a type 2N128 transistor.

The comparison of Z_{01} and Z_{03} is of most interest because the difference between them is mainly due to the effects of the complex quantity $(1-\alpha)$. At frequencies lower than f_α, Eq. (7.1) reduces to:

$$Z_{01} \approx Z_c \quad . \tag{7.4}$$

Comparing Eqs. (7.3) and (7.4),

$$Z_{03} = Z_{01}(1-\alpha) \quad , \tag{7.5}$$

where

$$Z_{01} = |Z_{01}| \angle\theta_1 \quad ,$$

$$Z_{02} = |Z_{02}| \angle\theta_2 \quad , \text{ and}$$

$$(1-\alpha) = |1-\alpha| \angle\theta_{(1-\alpha)} \quad .$$

The absolute magnitude of Z_{03} then is:

$$|Z_{03}| = |Z_{01}| \times |1-\alpha| \quad , \tag{7.6}$$

and the phase angle of Z_{03} is:

$$\theta_3 = \theta_1 + \theta_{(1-\alpha)} \quad . \tag{7.7}$$

It is desirable at this point to study the nature of the quantity $(1-\alpha)$ as related to the complex form of α:

$$\alpha = \frac{a_0}{1 + j(\omega/\omega_\alpha)} \quad . \tag{7.8}$$

If a vector plot of α versus frequency is made using polar coordinates, the form will be as shown in Fig. 7.5.[4]

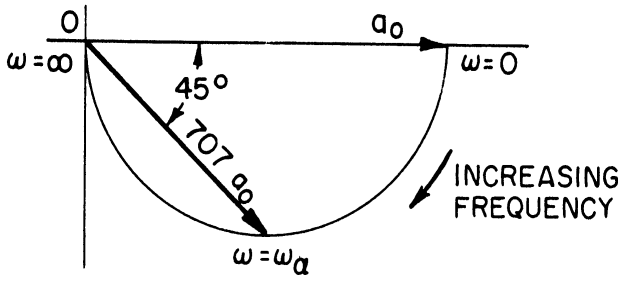

Fig. 7.5. Vector plot of α versus radian frequency.

A translation can be performed which will allow the vector $(1-\alpha)$ to be represented also as in Fig. 7.6. A value of $a_0 = .9$ was chosen for convenience. The vector $(1-\alpha)$ originates at the origin and terminates at some point on the left-hand semicircle.

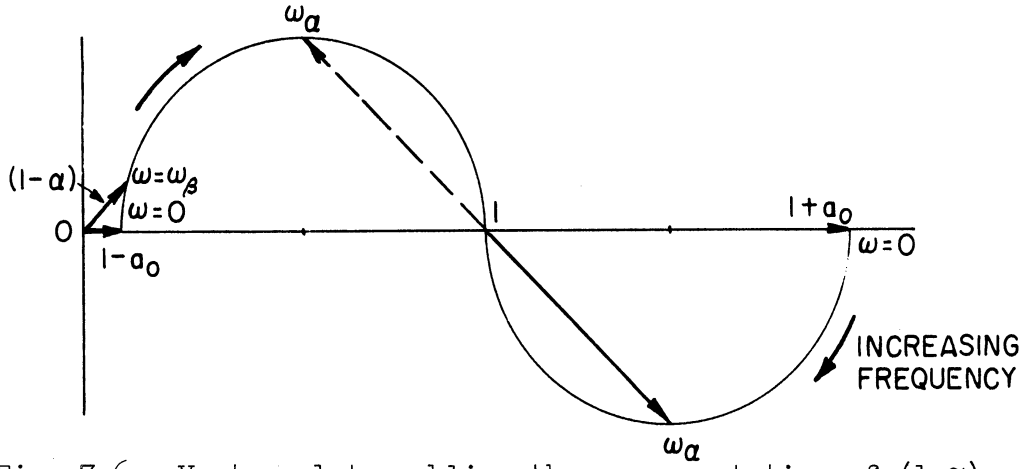

Fig. 7.6. Vector plot enabling the representation of $(1-\alpha)$.

In general, the grounded emitter current gain is:

$$\beta = \frac{\alpha}{1-\alpha} \quad , \quad b_0 = \frac{a_0}{1-a_0} \quad . \tag{7.9}$$

At frequencies lower than that at which β decreases to .707 times its zero-fre-

quency value, it is valid to say:

$$\beta \approx \frac{a_o}{1-\alpha} \quad . \tag{7.10}$$

From Eq. (7.10) it is seen that the frequency f_β (at which β decreases to .707 b_o) will occur at the point where $(1-\alpha)$ has increased in magnitude to $\sqrt{2}(1-a_o)$. The radian frequency ω_β is shown in Fig. 7.6 and an enlarged view is shown in Fig. 7.7.

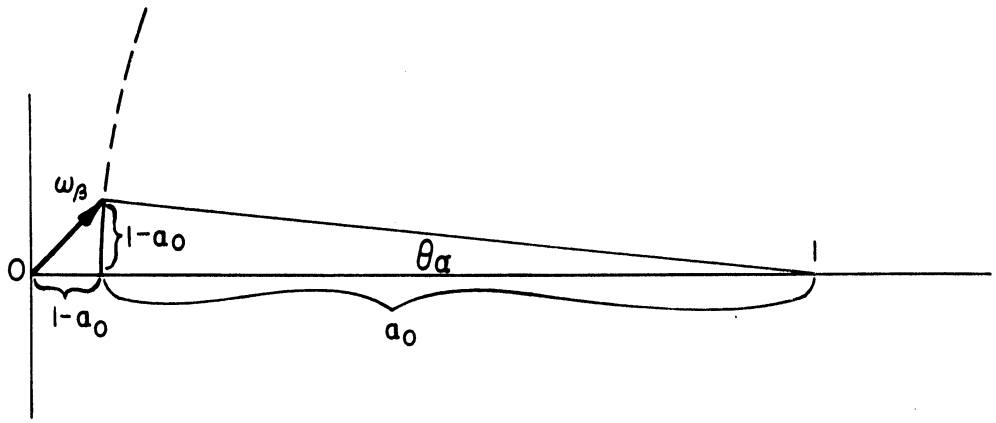

Fig. 7.7. Enlarged view of Fig. 7.6 showing the conditions for $\omega = \omega_\beta$.

From Eq. (7.8), when $\omega = \omega_\beta$, the magnitude of θ_α, which is the phase angle of α, is:

$$\theta_\alpha = \text{arc tan} \frac{\omega_\beta}{\omega_\alpha} \quad . \tag{7.11}$$

Also from Fig. 7.7, for magnitudes of a_o close to unity

$$\theta_\alpha \approx \text{arc tan} \frac{1-a_o}{a_o} \quad ; \tag{7.12}$$

then

$$\omega_\beta \approx \frac{1-a_o}{a_o} \omega_\alpha = \frac{\omega_\alpha}{b_o} \quad . \tag{7.13}$$

By comparing the curves of Z_{o1} and Z_{o3}, an indication of the magnitude and phase of $(1-\alpha)$ is obtainable at any frequency in the range of measurement. From Eqs. (7.6) and (7.7):

$$|1-\alpha| = \frac{|Z_{o3}|}{|Z_{o1}|} \quad \text{and} \tag{7.14}$$

$$\theta_{(1-\alpha)} = \theta_3 - \theta_1 \quad . \tag{7.15}$$

The frequency at which the grounded emitter current gain β drops 3 db should correspond to the point at which $\theta_{(1-\alpha)} = 45°$. f_β can thus be determined and if b_o is known, it is possible to predict f_α as from Eq. (7.13):

$$f_\alpha = b_o f_\beta \quad . \tag{7.16}$$

Using the curves of Z_{o1} and Z_{o3} in Figs. 7.2 and 7.4, $\theta_{(1-\alpha)} = 45°$ at f_β = 2 mcs.

The magnitude b_o calculated from the low-frequency characteristics was 40; thus the predicted f_α would be 2 x 40 = 80 mcs. This frequency is high for a type 2N128 transistor, but using the same technique on another of the same type yielded f_β = 1.7 mcs, b_o = 38 for a predicted f_α = 65 mcs. These results are in closer agreement with nominal values. It is clear in the above cases that f_β must be known very accurately to expect a good approximation of f_α. The same accuracy can be required of b_o as proves to be the case when measurements were made of the type GA53233 diffused base transistor. A test yielded f_β = 65 mcs and a value of $(1-\alpha) = 1/6 \ \underline{/4°}$ at 4 mcs. The phase shift at this frequency is negligible and so this value of $(1-\alpha)$ is essentially $1-a_o = 1/1+b_o$; thus the magnitude of $(1+b_o)$ is 6 and b_o = 5. The predicted f_α for this transistor is then f_α = 5 x 65 = 325 mcs. In this case, an error in the measurement of b_o will have a considerably larger effect than an error in the measurement of f_β in the prediction of f_α. Moreover, it was noted that the value of b_o as calculated from the absolute impedance ratio ($b_o \approx 5$) did not coincide with the value as calculated from the static characteristics ($b_o \approx 8$). The dynamic value as computed from the impedance ratio is undoubtedly a better approximation but some uncertainty does remain.

The reason for including the curve of Z_{o2} is that the difference between it and the curve of Z_{o3} is due mainly to the relative magnitudes of r_e and r_b'. It can be seen, for example, that if r_b' were much greater than r_e in Eq. (7.2), Z_{o2} would approximately equal $Z_c(1-\alpha)$, which is the relationship for Z_{o3}. Since the difference between Z_{o2} and Z_{o3} can be computed from measurements, the value of r_b' will be calculated as a function of Z_{o1}, Z_{o2}, Z_{o3}, and r_e. Using Eqs. (7.1), (7.2), and (7.3) and restricting the applicability to lower frequencies where the phase shift of $(1-\alpha)$ is negligible, i.e., where the impedances Z_{o1}, Z_{o2}, and Z_{o3} have a common phase shift:

$$\text{dividing } Z_{o3} \text{ by } Z_{o1}, \qquad 1 - \alpha = \frac{Z_{o3}}{Z_{o1}} \ ; \tag{7.17}$$

$$\text{dividing } Z_{o2} \text{ by } Z_{o1}, \qquad 1 - \frac{\alpha \, r_b'}{r_e + r_b'} = \frac{Z_{o2}}{Z_{o1}} \quad . \tag{7.18}$$

Solving Eqs. (7.17) and (7.18) simultaneously for r_b',

$$r_b' = r_e \frac{Z_{o1} - Z_{o2}}{Z_{o2} - Z_{o3}} \quad . \tag{7.19}$$

In a test it must be assured that the emitter current is constant for all three impedances; then $r_e \approx 25.7/I_e(ma)$ for germanium transistors. Values calculated for r_b' were 192 ohms for a type 2N128 transistor and 7.2 ohms for a type GA53233. A value for the same type 2N128 transistor calculated another way, to be discussed in the following section, was 190 ohms.

Further analysis in the use of measurements of Z_{o1}, Z_{o2}, and Z_{o3} should prove more conclusively the validity of what has been presented in this section, and will examine frequencies above f_β to determine how well the theoretical relationships for α and $(1-\alpha)$ predict the actual circumstances.

8. FURTHER DEVELOPMENT OF THE OUTPUT IMPEDANCE OF THE GROUNDED BASE CONFIGURATION

Further study of the output impedance of the grounded base configuration has led to methods of obtaining C_c and r_b'. Under the conditions of large input impedance, from Eq. (6.7):

$$Z_o \approx Z_c + r_b' \quad . \tag{8.1}$$

Assuming constant values for C_c, r_c, and r_b' the circuit representation and the equivalent as seen by the RX meter are shown in Figs. 8.1a and 8.1b.

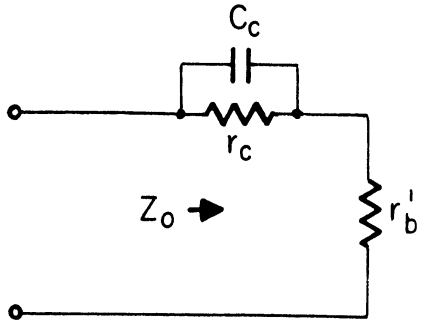

Fig. 8.1a. Representation of the transistor grounded base output impedance.

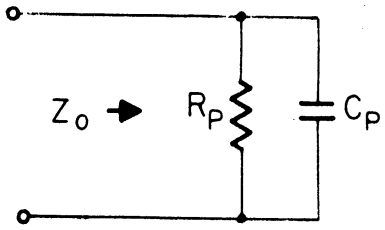

Fig. 8.1b. Equivalent representation as seen by RX meter.

Because the magnitude of r_c is ordinarily much greater than X_{C_c} at the frequencies of interest, the $r_b'C_c$ time constant will be of primary concern in the development below.

The derived relationships between the transistor parameters and the parallel components in the equivalent representation are:

$$Rp = \frac{(r_c+r_b')^2 + r_c^2(\omega/\omega_o)^2}{r_c+r_b' + \frac{r_c^2}{r_b'}(\omega/\omega_o)^2} , \quad \omega_o = \frac{1}{r_b'C_c} , \tag{8.2}$$

$$Cp = \frac{r_c^2 C_c}{(r_c+r_b')^2 + r_c^2(\omega/\omega_o)^2} . \tag{8.3}$$

Under the circumstances that

$$r_c \gg r_b' ,$$

the parallel components can be simplified as follows:

$$Rp \approx r_c \frac{1 + (\omega/\omega_o)^2}{1 + \frac{r_c}{r_b'}(\omega/\omega_o)^2} , \quad \omega_o = \frac{1}{r_b'C_c} , \tag{8.4}$$

$$Cp \approx C_c \frac{1}{1 + (\omega/\omega_o)^2} . \tag{8.5}$$

At very low frequencies where $r_c/r_b'(\omega/\omega_o)^2 \ll 1$, the value of r_c can be measured directly as equal to Rp. This condition is not as easily met as it might seem because of the factor r_c/r_b'. For example, typical values of r_c and r_b' are 10^6 and 10^2 ohms, respectively, and thus a typical ratio is $r_c/r_b' = 10^4$. Then in order to measure r_c directly, $\omega \ll \sqrt{10^{-4}}\ \omega_o$. Therefore, in the example, the radian frequency of measurement must be 10^{-3} times the radian frequency associated with the $r_b'C_c$ time constant to expect a possible accuracy of 1% in the direct measurement of r_c.

The restrictions are not nearly as severe if direct measurement of C_c is desired. From Eq. (8.5) it can be seen that if $\omega = 0.1\ \omega_o$, the assumption that C_c is equal to Cp will be correct within 1%.

For other ratios of r_c/r_b' the relationships are not the same as for the typical example; however, information concerning these ratios can be easily obtained if various curves are drawn for the normalized quantity Rp/r_b' versus ω/ω_o for expected ratios of r_c/r_b'. From Eq. (8.4):

$$\frac{Rp}{r_b'} = \left(\frac{r_c}{r_b'}\right) \frac{1 + (\omega/\omega_o)^2}{1 + \frac{r_c}{r_b'}(\omega/\omega_o)^2} = \frac{1 + (\omega/\omega_o)^2}{\frac{r_b'}{r_c} + (\omega/\omega_o)^2} . \tag{8.6}$$

From Eq. (8.5):

$$\frac{Cp}{C_c} = \frac{1}{1 + (\omega/\omega_o)^2} . \tag{8.7}$$

Curves of Rp/r_b' (for four different ratios of r_c/r_b') and of Cp/C_c versus ω/ω_o are shown in Fig. 8.2.

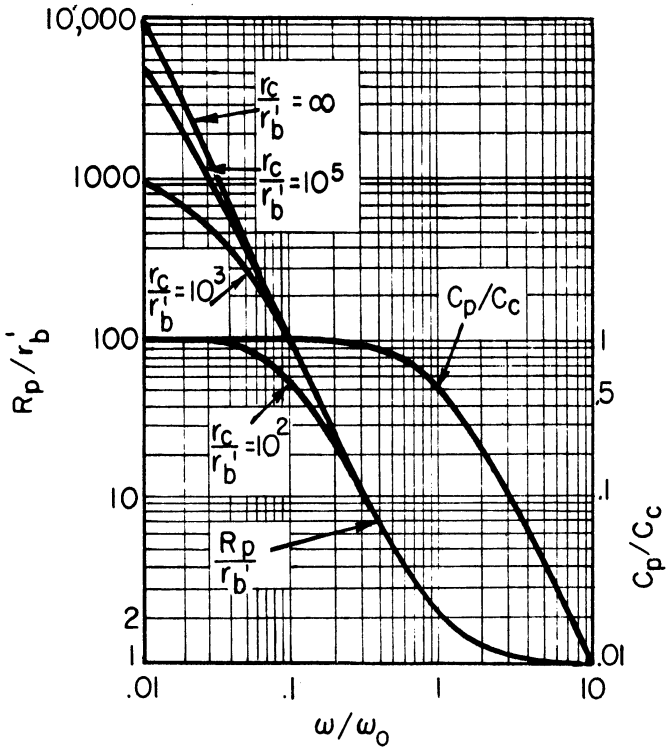

Fig. 8.2. Curves of Rp/r_b' and Cp/C_c versus ω/ω_o.

It can be seen from Eqs. (8.6) and (8.7) or from Fig. 8.2 that for $\omega/\omega_o = 1$:

$$Rp/r_b' \approx 2, \quad \omega/\omega_o = 1 \quad , \tag{8.8}$$

$$Cp/C_c = 1/2, \quad \omega/\omega_o = 1 \quad . \tag{8.9}$$

These conditions allow determination of r_b' and ω_o. Once the low-frequency value of C_c is known, the frequency of measurement can be increased until $Cp \approx 1/2\ C_c$; and at this point, the radian frequency is equal to:

$$\omega_o = \frac{1}{r_b' C_c} \quad , \tag{8.10}$$

Since C_c is known, r_b' can be obtained directly:

$$r_b' = \frac{1}{\omega_o C_c} \quad . \tag{8.11}$$

Alternatively, since resistance measurements have been made at this critical frequency:

$$r_b' = \frac{Rp}{2} \quad . \tag{8.12}$$

r_b' can thus be calculated from two interdependent relationships, one value obtained serving as a check upon the other.

Impedance measurements were made using several different types of transistors and the values for $1/\omega_o$, r_b', and C_c are tabulated in Fig. 8.3.

Transistor	$1/\omega_o = r_b'C_c$	C_c	$r_b' = \frac{1}{\omega_o C_c}$	$r_b' = \frac{Rp}{2}$
	μμsec	μμfd	ohms	ohms
2N129	1225	5	245	260
2N128	935	4.9	190	200
2N393	500	4.2	119	120
2N300	295	3.2	92	90
GA53233	<100	5	---	---

Fig. 8.3. Table of $r_b'C_c$, C_c, and r_b' for various transistors.

Measurements were not obtainable for the 2N393 and 2N300 above 250 mcs, but there was enough information to estimate the values shown because the slope of the Cp-versus-frequency curve allowed extrapolation to the frequency of interest. The maximum frequency of measurement was 250 mcs which corresponds to the minimum certain $r_b'C_c$ time of 636 μμsec if the Boonton RX meter is used. If a method were devised to measure C_c alone at frequencies higher than 250 mcs, a good indication of the critical ω_o and thus r_b' should still be obtainable.

Two effects that have not been discussed concerning the measurement of output impedance of the grounded base configuration are: (1) the resistance Rp reading starts at some finite value and then increases with an increase in the frequency of measurement to higher than the "infinity" mark (as indicated on the dial of the RX meter), and (2) the capacitance Cp reading increases slightly to a maximum value with frequency just before the expected slope towards the $1/2\ C_c$ value takes place. The increase in effective resistance is evidently due to regenerative feedback through the collector emitter capacitance developed across the high input impedance, and occurs at frequencies much lower than the critical frequency:

$$f_o = \frac{1}{2\pi r_b'C_c} .$$

The increase in capacitance is evidently due to the internal characteristics of the transistor itself.

9. THE GROUNDED COLLECTOR CONFIGURATION

Measurements have not yet been made and the capabilities not thoroughly studied but first indications are that both input and output impedance of the grounded collector configuration should yield valuable information.

From Eq. (6.15):

$$Z_i \approx r_b' + \frac{Z_c R_L (1+\beta)}{Z_c + R_L (1+\beta)} , \qquad R_L > r_e . \tag{9.1}$$

The synthesis of (9.1) appears in Fig. 9.1:

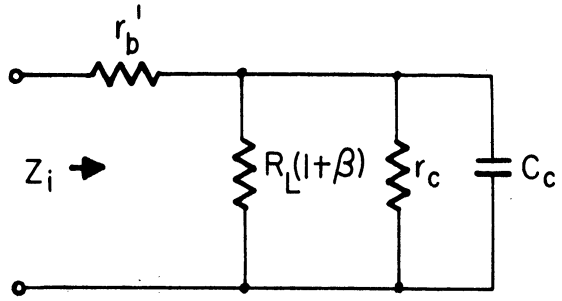

Fig. 9.1. Representation of the grounded collector input impedance.

From Eq. (6.16), the output impedance for a resistive input impedance is:

$$Z_o \approx r_e + \frac{r_b + r_g}{1 + \beta} . \tag{9.2}$$

Here is a relationship which allows an increasing value of Z_o as the quantity $(1+\beta)$ decreases with frequency. Thus the accuracy of measurement should be good at high frequencies and the phase shift involved should be due principally to β.

10. FUTURE PLANS

It is planned to continue work on the system of impedance measurement techniques. The output impedance of the grounded emitter configuration will be analyzed at frequencies above f_β, and the capabilities of the grounded collector configurations will be studied.

11. REFERENCES

1. Giacoletto, L. J., "Terminology and Equations for Linear Active Four Terminal Networks Including Transistors," RCA Review, 14, 28-46 (March, 1953).

2. Middlebrook, R. D., An Introduction to Junction Transistor Theory (John Wiley and Sons, Inc., New York, 1957), pp. 237-255.

3. Shea, R. F., Principles of Transistor Circuits (John Wiley and Sons, Inc., New York, 1953), Chs. 9-10.

4. Ibid., p. 205.

PART II

GAS-TUBE STUDY

Cold-Cathode Breakdown Study

The present objective of the gas-tube study is to obtain maximum familiarity with the effects of the various gaseous conduction parameters, including the geometry, on the volt-ampere behavior of Townsend current flow at very small currents. Interest will eventually be centered about the transient change from Townsend-current to glow discharge or arc behavior. The integral equations describing the volt-ampere and transient behavior must take into account the field distortion produced by space charge and the effect of this distortion upon the various condition parameters such as the first and second Townsend coefficients and the ionic mobility.

The initial phase of the work has consisted of a critical study of the origin of the general integral equation governing Townsend current phenomena under operating conditions for which space charge causes important field distortion. The equation was studied assuming a one-dimensional system which may be either planar or cylindrical.

After obtaining an appropriate form for this equation, an extensive study of the literature was made to permit estimation of a reasonable functional dependence of the gaseous conduction parameters α, r, and ionic mobility. It is well known that although adequate empirical equations for these parameters may be obtained for any restricted range of electric field and gas pressure, it is not legitimate to assign any particular functional dependence over an extended range. For example, although mobility is constant at low fields, it becomes dependent upon the electric field at high fields. Because of this variability of the various parameters with the field, the solution of the integral equation requires numerical or analog computer techniques. Analog computer techniques seem appropriate because of the speed and flexibility they offer for studies in which the objective is to gain maximum familiarity with gross behavior. Analog solutions are currently being obtained and will be presented and discussed in a subsequent technical report.